

# Vibrational structure and symmetry in $^{110-116}\text{Cd}$ \*

A. LEVIATAN

Racah Institute of Physics, The Hebrew University, Jerusalem 91904, Israel

J.E. GARCÍA-RAMOS

Department of Integrated Sciences and Center for Advanced Studies in Physics,  
Mathematics and Computation, University of Huelva, 21071 Huelva, Spain

N. GAVRIELOV, P. VAN ISACKER

Grand Accélérateur National d'Ions Lourds, CEA/DRF-CNRS/IN2P3,  
Bvd Henri Becquerel, BP 55027, F-14076 Caen, France

We show that a vibrational interpretation and good  $U(5)$  symmetry are maintained for the majority of low-lying normal states in  $^{110,112,114,116}\text{Cd}$  isotopes, consistent with the empirical data. The observed deviations from this paradigm are properly treated by an interacting boson model Hamiltonian which breaks the  $U(5)$  symmetry in selected non-yrast states, while securing a weak mixing with coexisting  $SO(6)$ -like intruder states. The results demonstrate the relevance of the  $U(5)$  partial dynamical symmetry notion to this series of isotopes.

Even-even cadmium isotopes ( $Z=48$ ) near the neutron mid-shell, have traditionally been considered as textbook examples of spherical-vibrator motion and  $U(5)$  dynamical symmetry [1, 2, 3]. On the other hand, recent detailed studies using complementary spectroscopic methods, have provided evidence for marked deviations from such a structural paradigm [4, 5, 6, 7]. The low-lying spectra of these isotopes exhibit additional coexisting intruder states [8], associated with the promotion of two protons across the  $Z=50$  shell gap. Previous attempts to explain the observed discrepancies in  $E2$  decays relied on strong mixing between vibrational and intruder states, and ultimately proved unsuccessful [5, 6, 7]. This paradoxical behavior has led to claims for the breakdown of vibrational motion in the isotopes  $^{110-116}\text{Cd}$  [5] and defines the so-called “Cd problem” [8].

---

\* Presented at the 57th Zakopane Conference on Nuclear Physics, *Extremes of the Nuclear Landscape*, Zakopane, Poland, 25 August–1 September, 2024.

Two approaches have been proposed to address these unexpected findings. The first abandons the traditional spherical-vibrational interpretation of the Cd isotopes, replacing it with multiple shape coexistence of states in deformed bands, a view qualitatively supported by a beyond-mean-field calculation of  $^{110,112}\text{Cd}$  with the Gogny D1S energy density functional [9, 10]. A second approach is based on the recognition that the reported deviations from a spherical-vibrator behavior show up in selected non-yrast states, while most states retain their vibrational character. In the terminology of symmetry, this implies that the symmetry in question is broken only in a subset of states, hence is partial [11]. In the present contribution, we follow the latter approach and show that the empirical data in  $^{110-116}\text{Cd}$  is compatible with a vibrational interpretation and U(5) partial symmetry for normal states, weakly coupled to deformed SO(6)-like intruder states [12, 13].

A convenient starting point for describing vibrations of spherical nuclei is the U(5) dynamical symmetry (DS) limit of the interacting boson model (IBM) [2], corresponding to the following chain of nested algebras,

$$\text{U}(6) \supset \text{U}(5) \supset \text{SO}(5) \supset \text{SO}(3) . \quad (1)$$

The associated DS basis states  $|[N], n_d, \tau, n_\Delta, L\rangle$  are specified by quantum numbers which are the labels of irreducible representations of the algebras in the chain. Here  $N$  is the total number of monopole ( $s$ ) and quadrupole ( $d$ ) bosons,  $n_d$  and  $\tau$  are the  $d$ -boson number and seniority, respectively,  $L$  is the angular momentum and  $n_\Delta$  is a multiplicity label. The U(5)-DS Hamiltonian can be transcribed in the form

$$\begin{aligned} \hat{H}_{\text{DS}} = & \rho_1 \hat{n}_d + \rho_2 \hat{n}_d(\hat{n}_d - 1) + \rho_3 [-\hat{C}_{\text{SO}(5)} + \hat{n}_d(\hat{n}_d + 3)] \\ & + \rho_4 [\hat{C}_{\text{SO}(3)} - 6\hat{n}_d] , \end{aligned} \quad (2)$$

where  $\hat{C}_G$  is a Casimir operator of the algebra  $G$ , and  $\hat{n}_d = \sum_m d_m^\dagger d_m = \hat{C}_{\text{U}(5)}$ .  $\hat{H}_{\text{DS}}$  is completely solvable with eigenstates  $|[N], n_d, \tau, n_\Delta, L\rangle$  and energies  $E_{\text{DS}} = \rho_1 n_d + \rho_2 n_d(n_d - 1) + \rho_3 [-\tau(\tau + 3) + n_d(n_d + 3)] + \rho_4 [L(L + 1) - 6n_d]$ . The U(5)-DS spectrum resembles that of a spherical vibrator with states arranged in  $n_d$ -multiplets and strong  $(n_d + 1 \rightarrow n_d)$   $E2$  transitions with particular ratios, *e.g.*,  $\frac{B(E2; n_d+1, L'=2n_d+2 \rightarrow n_d, L=2n_d)}{B(E2; n_d=1, L=2 \rightarrow n_d=0, L=0)} = (n_d + 1) \frac{(N - n_d)}{N}$ .

As a typical example, the empirical spectrum of  $^{110}\text{Cd}$  shown in Fig. 1, consists of both normal and intruder levels. At first sight, the normal states seem to follow the expected pattern of spherical-vibrator  $n_d$ -multiplets. As seen in Table 1, the measured  $E2$  rates support this view for the majority of normal states, however, selected non-yrast states (shown in red in Fig. 1) reveal marked deviations from this behavior. Specifically, the  $0_3^+$  and  $2_5^+$  states in  $^{110}\text{Cd}$  (denoted in Table 1 by  $0_\alpha^+$  and  $2_\alpha^+$ ) which in the U(5)-DS

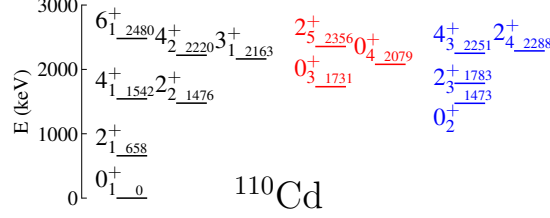


Fig. 1. Experimental spectrum of  $^{110}\text{Cd}$  in keV. Normal states are marked in black, or in red if their  $E2$  decays deviate from those of a spherical vibrator and  $U(5)$  dynamical symmetry. Intruder states are marked in blue. Data are taken from [14].

Table 1. Comparison between experimental (EXP) and  $U(5)$ -DS predicted  $B(E2; L_i \rightarrow L_f)$  values in Weisskopf units (W.u.) for normal states in  $^{110-116}\text{Cd}$ . The  $0_\alpha^+$  ( $2_\alpha^+$ ) state corresponds to the experimental  $0_3^+, 0_3^+, 0_3^+, 0_2^+$  ( $2_5^+, 2_4^+, 2_5^+, 2_4^+$ ) state for  $^A\text{Cd}$  ( $A = 110, 112, 114, 116$ ), respectively. In the  $U(5)$ -DS classification,  $(0_1^+, 2_1^+, 2_2^+, 4_1^+, 6_1^+)$  are the class-A states with  $n_d = 0, 1, 2, 2, 3$ , and  $(0_\alpha^+, 2_\alpha^+)$  are states with  $n_d = (2, 3)$ . Data are taken from [4, 5, 6, 7, 14].

$L_i \rightarrow L_f$	$^{110}\text{Cd}$		$^{112}\text{Cd}$		$^{114}\text{Cd}$		$^{116}\text{Cd}$	
	EXP	$U(5)$	EXP	$U(5)$	EXP	$U(5)$	EXP	$U(5)$
$2_1^+ \rightarrow 0_1^+$	27.0(8)	27.0	30.31(19)	30.31	31.1(19)	31.1	33.5(12)	33.5
$4_1^+ \rightarrow 2_1^+$	42(9)	46	63(8)	53	62(4)	55	56(14)	59
$2_2^+ \rightarrow 2_1^+$	30(5)	46	39(7)	53	22(6)	55	25(10)	59
$2_2^+ \rightarrow 0_1^+$	0.68(14)	0	0.65(11)	0	0.48(6)	0	1.11(18)	0
$6_1^+ \rightarrow 4_1^+$	40(30)	58		68	119(15)	72	$110^{+40}_{-80}$	75
$0_\alpha^+ \rightarrow 2_1^+$	$< 7.9$	46	0.0121(17)	53	0.0026(4)	55	0.79(22)	59
$0_\alpha^+ \rightarrow 2_2^+$	$< 1680$	0	99(16)	0	127(16)	0		0
$2_\alpha^+ \rightarrow 2_2^+$	$0.7^{+0.5}_{-0.6}$	11	$< 1.6^{+6}_{-4}$	13	$2.5^{+16}_{-14}$	14	2.0(6)	14
$2_\alpha^+ \rightarrow 0_\alpha^+$	24.2(22)	27	25(7)	32	17(5)	34	35(10)	35

classification are members of the  $n_d = 2$  and  $n_d = 3$  multiplets, respectively, have unusually small  $E2$  rates for the transitions  $0_\alpha^+ \rightarrow 2_1^+$  and  $2_\alpha^+ \rightarrow 2_2^+$ , and large rates for  $0_\alpha^+ \rightarrow 2_2^+$ , at variance with the  $U(5)$ -DS predictions. Absolute  $B(E2)$  values for transitions from the  $0_4^+$  state are not known, but its branching ratio to the  $2_2^+$  state is small [6]. As shown in Table 1, the same unexpected decay patterns occur in all cadmium isotopes with mass number  $A = 110-116$ , and comprise the above mentioned “Cd problem” [8]. We are thus confronted with a situation in which some states in the spectrum obey the predictions of  $U(5)$ -DS, while other states do not. These empirical

findings signal a potential role for a partial dynamical symmetry (PDS). In what follows, we show that an approach based on U(5) PDS provides a possible explanation for the Cd problem in these isotopes.

PDS-based approaches have been previously implemented in nuclear spectroscopy, in conjunction with the SU(3)-DS [15, 16, 17, 18], and SO(6)-DS [19, 20, 21, 22] chains of the IBM, relevant to axial and  $\gamma$ -soft deformed shapes, respectively. Here we focus on U(5)-PDS associated with the chain (1). The construction of Hamiltonians with U(5)-PDS follows the general algorithm [11, 20], by adding to the U(5)-DS Hamiltonian of Eq. (2), terms which annihilate particular sets of U(5) basis states. This leads to

$$\hat{H}_{\text{PDS}} = \hat{H}_{\text{DS}} + r_0 G_0^\dagger G_0 + e_0 (G_0^\dagger K_0 + K_0^\dagger G_0), \quad (3)$$

where  $G_0^\dagger = [(d^\dagger d^\dagger)^{(2)} d^\dagger]^{(0)}$  and  $K_0^\dagger = s^\dagger (d^\dagger d^\dagger)^{(0)}$ .  $G_0$  and  $K_0$  annihilate the states  $||N], n_d = \tau, \tau, n_\Delta = 0, L\rangle$  with  $L = \tau, \tau + 1, \dots, 2\tau - 2, 2\tau$  which, therefore, remain solvable eigenstates of  $\hat{H}_{\text{PDS}}$  with good U(5) symmetry. Henceforth, we refer to this special subset of states as class-A states. While  $\hat{H}_{\text{DS}}$  (2) is diagonal in the U(5)-DS chain (1), the  $r_0$  and  $e_0$  terms are not. Accordingly, the remaining eigenstates of  $\hat{H}_{\text{PDS}}$  (3) are mixed with respect to U(5) and SO(5). The U(5)-DS is therefore preserved in a subset of eigenstates but is broken in others. By definition,  $\hat{H}_{\text{PDS}}$  exhibits U(5)-PDS.

The combined effect of normal and intruder states, can be studied in the framework of the interacting boson model with configuration mixing (IBM-CM) [23, 24]. The latter is based on associating the different shell-model spaces of 0p-0h, 2p-2h, 4p-4h, ... particle-hole excitations, with the corresponding boson spaces comprising of  $N, N+2, N+4, \dots$  bosons, which are subsequently mixed. For two configurations, the IBM-CM Hamiltonian can be cast in matrix form,

$$\hat{H} = \begin{bmatrix} \hat{H}_{\text{normal}} & \hat{V}_{\text{mix}} \\ \hat{V}_{\text{mix}} & \hat{H}_{\text{intruder}} \end{bmatrix}, \quad (4)$$

where  $\hat{H}_{\text{normal}}$  represents the normal configuration ( $N$  boson space),  $\hat{H}_{\text{intruder}}$  represents the intruder configuration ( $N + 2$  boson space) and  $\hat{V}_{\text{mix}}$  is a mixing term. This procedure has been used extensively for describing co-existence phenomena in nuclei [25, 26, 27, 28].

In the present study,  $\hat{H}_{\text{normal}} = \hat{H}_{\text{PDS}}$ .  $\hat{H}_{\text{intruder}}$  contains quadrupole and rotational terms,  $\hat{H}_{\text{intruder}} = \kappa \hat{Q}_\chi \cdot \hat{Q}_\chi + \kappa' \hat{L} \cdot \hat{L} + \Delta$ , where  $\hat{Q}_\chi = d^\dagger s + s^\dagger \tilde{d} + \chi (d^\dagger \tilde{d})^{(2)}$  and  $\Delta$  an energy offset. The mixing term is  $\hat{V}_{\text{mix}} = \alpha [(s^\dagger)^2 + (d^\dagger d^\dagger)^{(0)}] + \text{H.c.}$ , where H.c. means Hermitian conjugate. The eigenstates  $|\Psi; L\rangle$  of  $\hat{H}$  (4), involve a mixture of normal ( $\Psi_n$ ) and intruder

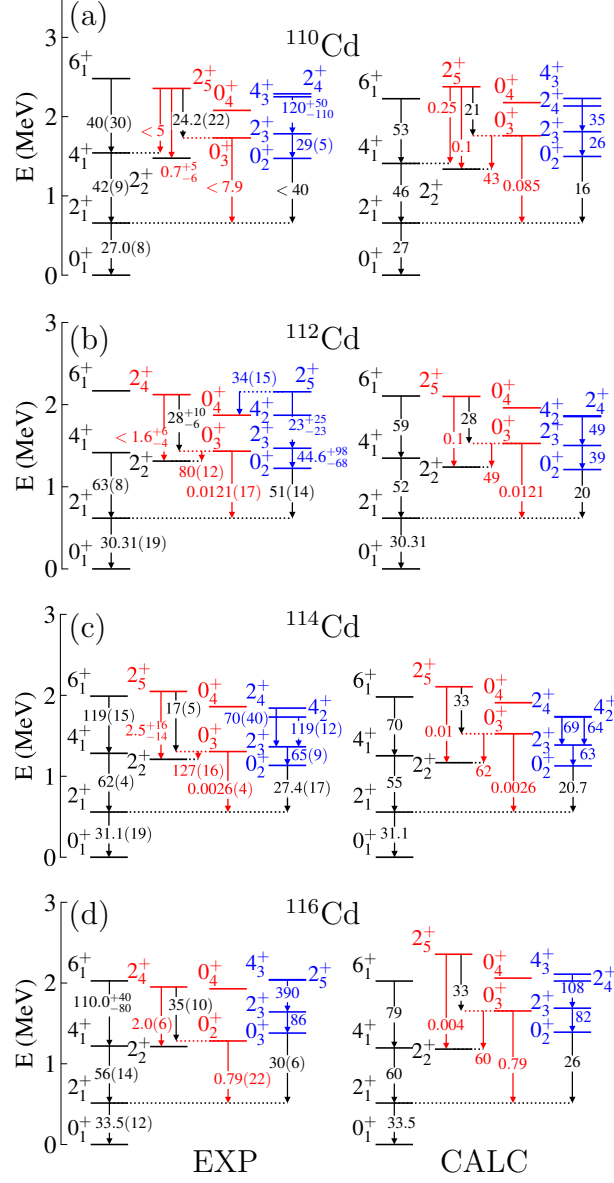


Fig. 2. Experimental (EXP) and calculated (CALC) energy levels in MeV and selected  $E2$  transition rates in W.u. for (a)  $^{110}\text{Cd}$ , (b)  $^{112}\text{Cd}$ , (c)  $^{114}\text{Cd}$ , (d)  $^{116}\text{Cd}$ . The parameters of the PDS-CM Hamiltonian (4) and  $E2$  transition operator employed in the calculation, are given in [13].

Table 2. Comparison between experimental (EXP) and U(5)-PDS calculated  $B(E2; L_i \rightarrow L_f)$  values in W.u. for normal levels in  $^{110-116}\text{Cd}$ . Notation of states as in Table 1.

$L_i \rightarrow L_f$	$^{110}\text{Cd}$		$^{112}\text{Cd}$		$^{114}\text{Cd}$		$^{116}\text{Cd}$	
	EXP	PDS	EXP	PDS	EXP	PDS	EXP	PDS
$2_1^+ \rightarrow 0_1^+$	27.0(8)	27.0	30.31(19)	30.31	31.1(19)	31.1	33.5(12)	33.5
$4_1^+ \rightarrow 2_1^+$	42(9)	46	63(8)	52	62(4)	55	56(14)	60
$2_2^+ \rightarrow 2_1^+$	30(5)	45	39(7)	51	22(6)	53	25(10)	59
$2_2^+ \rightarrow 0_1^+$	0.68(14)	0.0	0.65(11)	0.0	0.48(6)	0.0	1.11(18)	0.0
$6_1^+ \rightarrow 4_1^+$	40(30)	53		59	119(15)	70	$110^{+40}_{-80}$	79
$0_\alpha^+ \rightarrow 2_1^+$	$< 7.9$	0.08	0.0121(17)	0.0121	0.0026(4)	0.0026	0.79(22)	0.79
$0_\alpha^+ \rightarrow 2_2^+$	$< 1680$	43	99(16)	49	127(16)	61		60
$2_\alpha^+ \rightarrow 2_2^+$	$0.7^{+0.5}_{-0.6}$	0.124	$< 1.6^{+6}_{-4}$	0.08	$2.5^{+16}_{-14}$	0.005	2.0(6)	0.004
$2_\alpha^+ \rightarrow 0_\alpha^+$	24.2(22)	21	25(7)	28	17(5)	33	35(10)	33

$(\Psi_i)$  components in the  $[N]$  and  $[N+2]$  boson spaces,

$$|\Psi; L\rangle = a|\Psi_n; [N], L\rangle + b|\Psi_i; [N+2], L\rangle \quad , \quad a^2 + b^2 = 1 \quad . \quad (5)$$

The IBM-CM model space consists of  $[N] \oplus [N+2]$  boson spaces with  $N = 7, 8, 9$ , for  $^{110-114}\text{Cd}$ , respectively, and  $N = 8$  for  $^{116}\text{Cd}$ . The normal configuration corresponds in the shell model to having two proton holes below the  $Z = 50$  shell gap, and the intruder configuration corresponds to two-proton excitation from below to above this gap, creating 2p-4h states.

As shown in Fig. 2 and Table 2, the U(5)-PDS calculation of spectra and  $E2$  rates provides a good description of the empirical data in  $^{110-116}\text{Cd}$ . It yields the same  $B(E2)$  values as those of U(5)-DS for the class-A states  $(0_1^+, 2_1^+, 2_2^+, 4_1^+, 6_1^+)$ , and reproduces correctly the  $E2$  transitions involving the  $(0_\alpha^+, 2_\alpha^+)$  states which deviate considerably from the U(5)-DS predictions. The origin of these features is revealed by examining the structure of the eigenfunctions of  $\hat{H}$  (4), as discussed below.

Table 3 shows for states in the normal sector the percentage of the wave function within the normal configuration [the probability  $a^2$  of  $\Psi_n$  in Eq. (5)], and the dominant U(5)  $n_d$ -component in  $\Psi_n$  and its probability ( $P_{n_d}$ ). The class-A states  $(0_1^+, 2_1^+, 2_2^+, 4_1^+, 6_1^+)$ , are seen to be dominated by the normal component  $\Psi_n$  (large  $a^2 \geq 90\%$ ), implying a weak mixing (small  $b^2$ ) with the intruder states. The  $6_1^+$  state experiences a larger mixing consistent with its enhanced decay to the lowest  $4^+$  intruder state [7, 14]. The normal-intruder mixing increases with  $L$  for a given isotope, and increases towards mid-shell ( $^{114}\text{Cd}$ ), correlated with the decrease in energy of intruder states. The class-A states possess good U(5) quantum numbers to a good

Table 3. Configuration content and U(5) structure of the wavefunctions  $|\Psi, L\rangle$ , Eq. (5), of selected normal states, eigenstates of  $\hat{H}$ , Eq. (4). Shown are the probability ( $a^2$ ) of the normal part  $\Psi_n$ , the dominant  $n_d$  component in the U(5) decomposition of  $\Psi_n$ , and its probability  $P_{n_d}$  (in %).

	<sup>110</sup> Cd		<sup>112</sup> Cd		<sup>114</sup> Cd		<sup>116</sup> Cd	
$L_k^+$	$a^2$ (%)	$[(n_d) P_{n_d}]$	$a^2$ (%)	$[(n_d) P_{n_d}]$	$a^2$ (%)	$[(n_d) P_{n_d}]$	$a^2$ (%)	$[(n_d) P_{n_d}]$
$0_1^+$	98.23	[(0) 98.22]	97.94	[(0) 97.92]	97.98	[(0) 97.95]	98.27	[(0) 98.25]
$2_1^+$	96.38	[(1) 96.36]	95.10	[(1) 95.05]	95.28	[(1) 95.22]	96.84	[(1) 96.81]
$4_1^+$	90.73	[(2) 90.69]	83.19	[(2) 83.03]	83.05	[(2) 82.87]	92.95	[(2) 92.91]
$2_2^+$	89.81	[(2) 89.74]	81.62	[(2) 81.28]	78.77	[(2) 78.33]	91.31	[(2) 91.25]
$6_1^+$	71.18	[(3) 71.09]	42.92	[(3) 42.53]	39.46	[(3) 38.98]	79.34	[(3) 79.27]
$0_\alpha^+$	70.75	[(3) 70.46]	71.13	[(3) 69.54]	71.55	[(3) 70.79]	74.34	[(3) 74.14]
$2_\alpha^+$	68.34	[(4) 66.07]	65.89	[(4) 62.83]	40.78	[(4) 40.13]	55.68	[(4) 54.73]

Table 4. Configuration content and SO(6) structure of the wavefunctions  $|\Psi, L\rangle$ , Eq. (5), of selected intruder states, eigenstates of  $\hat{H}$ , Eq. (4). Shown are the probability ( $b^2$ ) of the intruder part  $\Psi_i$ , the dominant  $\sigma$  component in the SO(6) decomposition of  $\Psi_i$ , and its probability  $P_\sigma$  (in %). The  $0_{1;i}^+$ ,  $2_{1;i}^+$ ,  $2_{2;i}^+$  and  $4_{1;i}^+$  states, correspond to the experimental  $(0_2^+, 0_2^+, 0_2^+, 0_3^+)$ ,  $(2_3^+, 2_3^+, 2_3^+, 2_3^+)$ ,  $(2_4^+, 2_5^+, 2_4^+, 2_5^+)$  and  $(4_3^+, 4_2^+, 4_2^+, 4_3^+)$  states for  $^A\text{Cd}$  ( $A=110, 112, 114, 116$ ), respectively.

	<sup>110</sup> Cd		<sup>112</sup> Cd		<sup>114</sup> Cd		<sup>116</sup> Cd	
$L_{k;i}^+$	$b^2$ (%)	$[(\sigma) P_\sigma]$	$b^2$ (%)	$[(\sigma) P_\sigma]$	$b^2$ (%)	$[(\sigma) P_\sigma]$	$b^2$ (%)	$[(\sigma) P_\sigma]$
$0_{1;i}^+$	67.28	[(9) 67.11]	75.45	[(10) 75.29]	86.44	[(11) 86.33]	71.52	[(10) 71.30]
$2_{1;i}^+$	91.83	[(9) 91.60]	87.77	[(10) 87.44]	87.37	[(11) 87.00]	92.91	[(10) 92.75]
$2_{2;i}^+$	90.53	[(9) 90.15]	85.07	[(10) 84.49]	85.57	[(11) 84.99]	92.29	[(10) 91.99]
$4_{1;i}^+$	76.69	[(9) 76.13]	74.01	[(10) 73.43]	78.59	[(11) 77.98]	75.47	[(10) 74.83]

approximation. The U(5) decomposition of their  $\Psi_n$  part discloses a single  $n_d$  component with probability  $P_{n_d} \geq 90\%$  and  $n_d$ -values similar to the U(5)-DS assignments. Such a high  $n_d$ -purity is a characteristic feature of spherical type of states and U(5) dynamical symmetry.

The non-yrast  $0_\alpha^+$  and  $2_\alpha^+$  states are more susceptible to the normal-intruder mixing but still retain the dominance of the normal component  $\Psi_n$  ( $a^2 \sim 70\%$ ) and show a similar variation of the normal-intruder mixing, as a function of neutron number along the cadmium chain. However, in contrast to class-A states, their U(5) structure changes dramatically. Specifically, as is evident from Table 3, the  $\Psi_n$  parts of the  $0_\alpha^+$  and  $2_\alpha^+$  states, which in the U(5)-DS classification have  $n_d = 2$  and  $n_d = 3$ , have now dominant components with  $n_d = 3$  and  $n_d = 4$ , respectively. The change  $n_d \mapsto (n_d + 1)$

ensures weak ( $\Delta n_d = 2$ ) transitions from these states to class-A states, but secures strong  $2_\alpha^+ \rightarrow 0_\alpha^+$  ( $\Delta n_d = 1$ ) transitions, in agreement with the data shown in Table 2.

While the class-A and  $(0_\alpha^+, 2_\alpha^+)$  states are predominantly spherical, the intruder states are members of a single deformed band exhibiting a  $\gamma$ -soft spectrum, with characteristic  $0^+$ ,  $2^+$ ,  $(4^+, 2^+)$ , grouping of levels, shown in Fig. 2. Such a pattern resembles that encountered in the SO(6)-DS limit of the IBM, associated with the chain  $U(6) \supset SO(6) \supset SO(5) \supset SO(3)$  and related basis states  $||N], \sigma, \tau, n_\Delta, L\rangle$ . Table 4 shows for states in the intruder sector the percentage of the wave function within the intruder configuration [the probability  $b^2$  of  $\Psi_i$  in Eq. (5)], and the dominant SO(6)  $\sigma$ -component in  $\Psi_i$  and its probability ( $P_\sigma$ ). The intruder states are seen to have small mixing with the normal states (large  $b^2$ ). Their wavefunctions exhibit a broad  $n_d$ -distribution, as expected for deformed type of states, and a pronounced SO(6) quantum number,  $\sigma = N+2$ , albeit with a slight breaking of SO(5) symmetry induced by the quadrupole term in  $\hat{H}_{\text{intruder}}$ , Eq. (4).

In summary, the results reported in the present contribution suggest that the vibrational interpretation and related U(5) dynamical symmetry description of  $^{110-116}\text{Cd}$ , can be salvaged by considering a Hamiltonian with U(5)-PDS acting in the normal sector of spherical states with weak coupling to the intruder sector of SO(6)-like deformed states.

## REFERENCES

- [1] A. Bohr and B. R. Mottelson, *Nuclear Structure. II Nuclear Deformations* (Benjamin, New York, 1975).
- [2] F. Iachello and A. Arima, *The Interacting Boson Model* (Cambridge University Press, Cambridge, 1987).
- [3] R. F. Casten, *Nuclear Structure from a Simple Perspective* (Oxford University Press, Oxford, 2000).
- [4] P. E. Garrett, K. L. Green, H. Lehmann, J. Jolie, C. A. McGrath, M. Yeh and S. W. Yates, Phys. Rev. C **75**, 054310 (2007).
- [5] P. E. Garrett, K. L. Green and J. L. Wood, Phys. Rev. C **78**, 044307 (2008).
- [6] P. E. Garrett and J. L. Wood, J. Phys. G **37**, 064028 (2010); 069701 (2010).
- [7] P. E. Garrett, T. R. Rodríguez *et al.*, Phys. Rev. C **86**, 044304 (2012).
- [8] K. Heyde and J. L. Wood, Rev. Mod. Phys. **83**, 1467 (2011).
- [9] P. E. Garrett, T. R. Rodríguez, A. D. Varela, K. L. Green *et al.*, Phys. Rev. Lett. **123**, 142502 (2019).
- [10] P. E. Garrett, T. R. Rodríguez, A. Diaz Varela, K. L. Green *et al.*, Phys. Rev. C **101**, 044302 (2020).
- [11] A. Leviatan, Prog. Part. Nucl. Phys. **66**, 93 (2011).



- [12] A. Leviatan, N. Gavrielov, J. E. García-Ramos and P. Van Isacker, Phys. Rev. C **98**, 031302(R) (2018).
- [13] N. Gavrielov, J. E. García-Ramos, P. Van Isacker and A. Leviatan, Phys. Rev. C **108**, L031305 (2023).
- [14] Evaluated Nuclear Structure Data File (ENSDF), [www.nndc.bnl.gov/ensdf/](http://www.nndc.bnl.gov/ensdf/).
- [15] A. Leviatan, Phys. Rev. Lett. **77**, 818 (1996).
- [16] A. Leviatan, J. E. García-Ramos and P. Van Isacker, Phys. Rev. C **87**, 021302(R) (2013).
- [17] A. Leviatan and D. Shapira, Phys. Rev. C **93**, 051302(R) (2016).
- [18] A. Leviatan, Eur. Phys. J. Special Topics **229**, 2405 (2020).
- [19] A. Leviatan and P. Van Isacker, Phys. Rev. Lett. **89**, 222501 (2002).
- [20] J. E. García-Ramos, A. Leviatan and P. Van Isacker, Phys. Rev. Lett. **102**, 112502 (2009).
- [21] C. Kremer, J. Beller, A. Leviatan, N. Pietralla, G. Rainovski, R. Tripple and P. Van Isacker, Phys. Rev. C **89**, 041302(R) (2014).
- [22] P. Van Isacker, J. Jolie, T. Thomas and A. Leviatan, Phys. Rev. C **92**, 011301(R) (2015).
- [23] P. D. Duval and B. R. Barrett, Phys. Lett. B **100**, 223 (1981).
- [24] P. D. Duval and B. R. Barrett, Nucl. Phys. A **376**, 213 (1982).
- [25] M. Sambataro and G. Molnar, Nucl. Phys. A **376**, 201 (1982).
- [26] J. E. García-Ramos and K. Heyde, Phys. Rev. C **92**, 034309 (2015).
- [27] K. Nomura and J. Jolie, Phys. Rev. C **98**, 024303 (2018).
- [28] N. Gavrielov, A. Leviatan and F. Iachello, Phys. Rev. C **105**, 014305 (2022).